THE JOURNAL OF BIOLOGICAL CHEMISTRY VOL. 290, NO. 45, pp. 27345–27359, November 6, 2015

Mouse Siglec-1 Mediates *trans*-Infection of Surface-bound Murine Leukemia Virus in a Sialic Acid *N*-Acyl Side Chain-dependent Manner*

Received for publication, July 27, 2015, and in revised form, September 2, 2015 Published, JBC Papers in Press, September 14, 2015, DOI 10.1074/jbc.M115.681338

Elina Erikson,[a,b,1] Paul R. Wratil,[c] Martin Frank,[d] Ina Ambiel,[a] Katharina Pahnke,[e] Maria Pino,[f] Parastoo Azadi,[g] Nuria Izquierdo-Useros,[f,2] Javier Martinez-Picado,[f,h] Chris Meier,[e] Ronald L. Schnaar,[i] Paul R. Crocker,[j] Werner Reutter,[c] and Oliver T. Keppler[a,b,3]

From the [a]Institute of Medical Virology, National Reference Center for Retroviruses, University of Frankfurt, 60596 Frankfurt am Main, Germany, the [b]Department of Infectious Diseases, Virology, University of Heidelberg, 69120 Heidelberg, Germany, the [c]Institut für Laboratoriumsmedizin, Klinische Chemie und Pathobiochemie, Charité Universitätsmedizin Berlin, 12200 Berlin, Germany, [d]Biognos AB, 402 74 Göteborg, Sweden, [e]Organic Chemistry, Department of Chemistry, Faculty of Sciences, University of Hamburg, 20146 Hamburg, Germany, the [f]AIDS Research Institute IrsiCaixa, Institut d'Investigatio en Ciencies de la Salut Germans Trias I Pujol, Universitat Autonoma de Barcelona, 08916 Barcelona, Spain, the [g]Complex Carbohydrate Research Center, University of Georgia, Athens, Georgia 30602, the [h]Institució Catalana de Recerca i Estudis Avançats (ICREA), 08010 Barcelona, Spain, the [i]Departments of Pharmacology and Neuroscience, The Johns Hopkins University School of Medicine, Baltimore, Maryland 21218, and the [j]College of Life Sciences, University of Dundee, Dundee DD1 5EH, Scotland, United Kingdom

Background: Human Siglec-1 mediates HIV *trans*-infection by interaction with virion-associated sialylated gangliosides.
Results: Here, Siglec-1 on mouse macrophages mediated *trans*-infection of surface-bound MLV. This could be inhibited by biosynthetic modification of sialic acids' *N*-acyl side chain in virus-producer cells.
Conclusion: The *N*-acyl side chain is a critical determinant of Siglec-1-dependent MLV *trans*-infection.
Significance: Glycoengineering allows manipulation of sialic acid-dependent virus/receptor interactions.

Siglec-1 (sialoadhesin, CD169) is a surface receptor on human cells that mediates *trans*-enhancement of HIV-1 infection through recognition of sialic acid moieties in virus membrane gangliosides. Here, we demonstrate that mouse Siglec-1, expressed on the surface of primary macrophages in an interferon-α-responsive manner, captures murine leukemia virus (MLV) particles and mediates their transfer to proliferating lymphocytes. The MLV infection of primary B-cells was markedly more efficient than that of primary T-cells. The major structural protein of MLV particles, Gag, frequently co-localized with Siglec-1, and *trans*-infection, primarily of surface-bound MLV particles, efficiently occurred. To explore the role of sialic acid for MLV *trans*-infection at a submolecular level, we analyzed the potential of six sialic acid precursor analogs to modulate the sialylated ganglioside-dependent interaction of MLV particles with Siglec-1. Biosynthetically engineered sialic acids were detected in both the glycolipid and glycoprotein fractions of MLV producer cells. MLV released from cells carrying *N*-acyl-modified sialic acids displayed strikingly different capacities for Siglec-1-mediated capture and *trans*-infection; *N*-butanoyl, *N*-isobutanoyl, *N*-glycolyl, or *N*-pentanoyl side chain modifications resulted in up to 92 and 80% reduction of virus particle capture and *trans*-infection, respectively, whereas *N*-propanoyl or *N*-cyclopropylcarbamyl side chains had no effect. In agreement with these functional analyses, molecular modeling indicated reduced binding affinities for non-functional *N*-acyl modifications. Thus, Siglec-1 is a key receptor for macrophage/lymphocyte *trans*-infection of surface-bound virions, and the *N*-acyl side chain of sialic acid is a critical determinant for the Siglec-1/MLV interaction.

The cellular lectin Siglec-1 and the sialyl-lactose-containing ganglioside, GM3, in the viral membrane were recently identified as critical determinants for HIV-1 particle capture and storage by human monocyte-derived dendritic cells (DCs)[4] as well as for DC-mediated *trans*-infection of T-cells (1). The term *trans*-infection refers to a two-step process as follows: the cap-

* This work was supported, in whole or in part, by National Institutes of Health Grant P41GM10349010 (Research Resource for Biomedical Glycomics to Complex Carbohydrate Research Center, University of Georgia) to P. A. and HL107151 to R. L. S. This work was also supported by the Robert Koch-Institute to the National Reference Center for Retroviruses (to O. T. K.), the Sonnenfeld-Stiftung Berlin (to W. R.), Spanish Secretariat for Research Grant SAF2013-49042-R (to N. I. U. and J. M. P.), and Goethe University (to O. T. K.). The authors declare that they have no conflicts of interest with the contents of this article.
[1] Present address: Dept. of Microbiology, Tumor and Cell Biology, Karolinska Institutet, 171 77 Stockholm, Sweden.
[2] Supported by Mathilde Krim Fellowship 108676 in basic biomedical research founded by "AmfAR," AIDS Research Foundation.
[3] To whom correspondence should be addressed: Institute of Medical Virology, National Reference Center for Retroviruses, University of Frankfurt, Paul-Ehrlich Str. 40, 60596 Frankfurt am Main, Germany. Tel.: 49-69-6301-5219; Fax: 49-69-6301-6477; E-mail: oliver.keppler@kgu.de.

[4] The abbreviations used are: DC, dendritic cell; MLV, murine leukemia virus; BMDM, bone marrow-derived macrophage; PDB, Protein Data Bank; mSiglec, mouse Siglec; But, *N*-butanoyl; iBut, *N*-isobutanoyl; Pent, *N*-pentanoyl; m.o.i., multiplicity of infection; ManNAc, *N*-acetyl-D-mannosamine; ManNProp, *N*-propanoyl-D-mannosamine; ManNBut, *N*-butanoyl-D-mannosamine; ManNiBut, *N*-isobutanoyl-D-mannosamine; ManNPent, *N*-pentanoyl-D-mannosamine; ManNCyclo, *N*-cyclopropylcarbamyl-D-mannosamine; ManNGc, *N*-glycolyl-D-mannosamine; Neu5G, *N*-glycolylneuraminic acid; ConA, concanavalin A; MD, molecular dynamics; Neu5Ac, *N*-acetylneuraminic acid; DMB, 1,2-diamino-4,5-methylenedioxybenzene·2HCl.

ture of virus particles by low or non-permissive cells that can retain viruses for a certain period and then mediate viral transmission to permissive neighboring target cells, promoting vigorous infection and spread (2). Siglec-1 is a transmembrane protein belonging to a family of sialic acid-binding immunoglobulin-like lectins. As a group-defining structural characteristic, Siglec proteins consist of an N-terminal V-set domain followed by a variable number of C2-set domains, a transmembrane domain, and a cytoplasmic tail (3). Characterizations of Siglec-1 in humans, mice, rats, and pigs indicate a preferential physiological expression of the lectin receptor on cells of the myeloid lineage. Its expression is mainly restricted to macrophage subsets, and in mice, it is highly exposed on macrophage subsets in the marginal zone of the spleen and in the subcapsular sinus of lymph nodes (4).

The physiological roles of Siglec-1 are still under debate. Although initially proposed to be a regulator of hematopoiesis (5–7), knock-out (KO) mice were viable, displayed no gross developmental abnormalities, and exhibited only subtle changes in B- and T-cell populations (8). Evidence is emerging that Siglec-1 may contribute to shaping various inflammatory and autoimmune responses (4). Furthermore, a role of Siglec-1 for infection, *trans*-infection, or clearance of sialylated pathogens other than HIV has been suggested (3, 9–11). Earlier work indicated a role of Siglec-1 as a receptor for infection of alveolar macrophages by porcine reproductive and respiratory syndrome virus. However, this was called into question in a study using Siglec-1 KO pigs (12). Both human and mouse Siglec-1 (mSiglec-1) expressed on human cells were recently shown to capture ecotropic murine leukemia virus (MLV), a simple retrovirus and mouse pathogen, in a ganglioside-dependent manner (13). Siglec-1 may also function as a recognition and uptake receptor for sialylated bacteria and protozoa, including *Neisseria meningitides, Campylobacter jejuni,* and *Trypanosoma cruzi* (4).

Siglec-1 binds promiscuously to a variety of sialylated molecules (9). For the lectin receptor the molecular basis of carbohydrate binding has been investigated by site-directed mutagenesis (14), crystallography (15), and nuclear magnetic resonance analysis (16). Accordingly, within the critical V-set domain of Siglec-1, arginine 97 and tryptophans at positions 2 and 106 were identified as key residues interacting with sialic acid. Siglec-1 has a preference for *N*-acetylneuraminic acid (Neu5Ac), the most abundant of the mammalian sialic acids, in α-2,3-linkage to D-galactose and does apparently not recognize Neu5Gc or Neu5Ac9Ac (17, 18). In line with these results, the sialylated carbohydrate headgroup of gangliosides constitutes the molecular recognition domain of HIV-1 particles as well as liposomes for human Siglec-1 (1). GM3 and possibly also GM2 gangliosides, all built of sialyl-lactose consisting of a sialic acid-D-galactose-D-glucose-trisaccharide linked to ceramide, appear to be critical for the HIV/Siglec-1 interaction (19, 20).

Reutter and co-workers and Bertozzi and co-workers (21, 22) identified biosynthetic engineering as an efficient tool to metabolically incorporate sialic acids with unnatural *N*-acyl side chains into cellular glycoconjugates. Synthetic *N*-acyl-modified D-mannosamines can be metabolized by the promiscuous sialic acid biosynthetic pathway and are incorporated into sialylated cell surface glycoconjugates replacing ~10–85% of natural sialic acids (23). This approach has enabled studies on sialic acid modifications in their native environment on the surface of living cells (24–27) as well as *in vivo* (16), and it has been exploited to introduce chemically reactive ketone or azide groups (22, 28).

In this study we analyzed the role of the lectin receptor mSiglec-1, endogenously expressed on primary macrophages, for capture of MLV and *trans*-infection of primary lymphocytes *ex vivo*. Furthermore, we explored whether metabolic engineering of sialic acids in virus-producer cells using synthetic *N*-acyl-modified precursor analogs is a feasible approach to modulate sialyl-lactose-containing gangliosides in released MLV particles and, importantly, whether this method can be used to assess the impact of *N*-substituted sialic acids on the functional interaction of viruses with mSiglec-1.

Experimental Procedures

Cell Culture—Cell lines S1A.TB.4.8.2 (S1A.TB; T-cell lymphoma from BALB/c mice), ANA-1 (myelomonocytic cell line established from bone marrow cells of C57BL/6 (H-2^b) mice infected with J2 recombinant retrovirus for immortalization), L929 cells (NCTC clone 929, subcutaneous areolar and adipose tissue of a 100-day-old male C3H/An mouse, secreting M-CSF), and 293T cells (human embryonic kidney cells) were obtained from the American Type Culture Collection and cultivated under standard conditions in Dulbecco's modified Eagle's medium or RPMI 1640 medium supplemented with 10% fetal bovine serum, 1% penicillin/streptomycin, and 1% L-glutamine (all from Gibco). The hybridoma producing rat anti-MLV Gag p30 antibody R184 was a kind gift from Dr. Carol Stocking.

Primary Mouse Cells—The generation of Siglec-1 KO mice on a C57BL/6 background has been reported (8). To prepare bone marrow-derived macrophages (BMDM), mice were sacrificed, and femur and tibia were extracted; bone marrow cells were collected by centrifugation and cultivated overnight in complete RPMI 1640 medium. Next, cells were seeded in BMDM differentiation medium containing 25% L929 supernatant as a source of colony-stimulating factor. 2–3 days later, fresh L929 supernatant was added to the cultures. Cells were reseeded for an experiment 6 days after preparation. For some experiments, 500 IU/ml mouse interferon α (IFNα, PBL Assay Science) was added 2 days prior to the experiment. Spleen and lymph nodes were placed in cold RPMI 1640 medium and gently passed through a 100-μm cell strainer. Cell suspensions were washed once in PBS, resuspended in complete RPMI 1640 medium, counted, and seeded in 96-well plates at a density of 5×10^6 cells/ml. In case of B- or T-cell activation, lipopolysaccharide (LPS, Sigma; 7.5 μg/ml) or concanavalin A (ConA, Sigma, 2 μg/ml) in combination with human interleukin 2 (IL-2, Biomol; 100 IU/ml) was added to the cultures.

Siglec-1 Genotyping—DNA was prepared from tail cuts of newborns using the DNeasy blood and tissue kit (Qiagen) according to the manufacturer's protocol for rodent tails. Following DNA extraction, a PCR, using allele-specific primers NEO (5′-CGTTGGCTACCCGTGATATTGC), SND1F3 (5′-CACCACGGTCACTGTGACAA), and SND2R2 (5′-GGCCATATGTAGGGTCGTCT), was performed in a thermocy-

cler (Eppendorf). PCR products were separated and visualized by agarose gel electrophoresis. The predicted sizes of diagnostic PCR products are as follows: WT(+/+), 495 bp; heterozygous(−/+), 495 and 204 bp; and homozygous KO(−/−), 204 bp.

Virus Preparation—The generation, production, and titration of MLV-GFP and MLV-Gag-GFP have been reported (29, 30).

Generation of MLV-GFP Particles in ManN Analog-treated 293T Cells—293T cells were seeded for virus production in the presence or absence of ManN analogs at non-toxic concentrations (5 mM for ManNAc, ManNProp, ManNBut, ManNiBut, ManNPent, and ManNCyclo or 0.3 mM for Ac_4ManNGc, Ac_4ManNAc, and Ac_4ManNProp). Peracetylated ManN derivatives were used to enhance membrane permeability. After entering the cell, the *O*-acetyl groups were cleaved by cytosolic esterases, releasing the active sialic acid precursors. After 5 days, cells were re-seeded and transfected with the MLV-GFP proviral plasmid. 4–6 h post-transfection, the medium was changed, and new ManN analogs were added. 48 h post-transfection, supernatants were collected, and viruses were purified by ultracentrifugation through a 20% sucrose cushion. All viral titers were determined on S1A.TB cells and identical titers were used in subsequent (*trans* or direct) infection experiments.

MLV Capture and Transfer Assays—To assess capture of MLV particles, L929-differentiated BMDM were incubated with MLV-GFP for 4 h at 37 °C and then washed extensively in PBS to remove unbound virus. BMDM were either analyzed for MLV $p30^{Gag}$ expression by intracellular flow cytometry using rat anti-MLV Gag p30 antibody R184, an Alexa488-conjugated donkey anti-rat antibody (Invitrogen), and the cytofix/cytoperm protocol (BD Biosciences) or for cell-associated MLV RT activity using a SYBR Green I-based product-enhanced RT assay, as reported previously (31).

In transfer experiments assessing Siglec-1-dependent transfer of MLV particles from macrophages to lymphocytes, BMDM or ANA-1 cells were incubated with virus particles according to the description above (in case of antibody blocking, BMDM were treated with 10 μg/ml anti-mSiglec-1 mAb (clone 3D6.112) or an isotype control mAb (Aviva Systems Biology) for 30 min at 4 °C before virus pulse). After extensive washing, either activated splenocytes or S1A.TB cells were added and co-cultured with macrophages in a ratio of 1:1 for 48 h. S1A.TB cells were harvested and analyzed for GFP expression; splenocytes were stained using phycoerythrin-conjugated anti-mCD19 and allophycocyanin-conjugated anti-mCD3 antibodies (BD Biosciences) and were acquired on a FACSVerse flow cytometer (BD Biosciences) using the FACSuite software and analyzed using FlowJo Software (Tree Star, Inc.).

Pronase Treatment—MLV-exposed BMDM were washed extensively in PBS and treated with increasing concentrations of Pronase (Roche Applied Science) for 30 min at 4 °C. Heat-inactivated Pronase that had been boiled for 10 min served as a control for the enzymatic activity. After extensive washing in medium containing FBS, target cells were added and co-cultured with macrophages in a ratio of 1:1 for 48 h. As an additional control to ensure that the Pronase treatment of the BMDM did not have any effect on splenocyte infectivity *per se*, a direct infection of LPS-activated splenocytes was carried out in BMDM supernatants that had been treated with Pronase, washed, and then incubated in medium for 1 h.

Immunofluorescence Microscopy—BMDM were seeded onto coverslips 1 day prior to the virus pulse. Washed cells were fixed in 4% paraformaldehyde/PBS for 30 min and then permeabilized with 0.1% Triton X-100/PBS for 2 min. Cells were blocked for 20 min in PBS containing 5% FCS, 0.1% BSA-c (Aurion), and 5% horse serum (Sigma). Cells were incubated with Alexa647-conjugated rat monoclonal anti-mouse Siglec-1 mAb 3D6.112 diluted in blocking buffer for 60 min at room temperature. Coverslips were mounted onto glass slides using DAPI mounting medium (Sigma). Epifluorescence images were acquired using a Nikon eclipse Ti-S microscope and the NIS-Elements imaging software. Acquired images were processed using ImageJ and Adobe Photoshop CS5.

Molecular Dynamics Simulations—Molecular dynamics simulations of Siglec-1 in complex with Neu5Ac, Neu5Gc, Neu5Prop, or Neu5But were performed in explicit solvent for 50 ns at 298 K using YASARA (29). The starting structures were built from the crystal structure of mouse Siglec-1 (PDB code 1OD7) by modifying the ligand using the YASARA graphical interface. Pressure control was performed by scaling the periodic simulation box to keep the water density at 0.997 g/liter. The AMBER03 (32) force field was used for the protein and GAFF parameters with AM1-BCC charges (33) for the carbohydrates. Long range Coulomb interactions were calculated using the Particle Mesh Ewald algorithm (34). Because the side chain of Arg-97 was flexible despite the presence of the ligand, a distance restraint of 100 newton/m was applied between the NH atoms of Arg-97 and the carboxylate oxygens of the ligands to maintain the hydrogen bonds. Simulation snapshots were recorded every 25 ps. The average interaction energy was calculated from all snapshots using a Yanaconda macro based on Equation 1,

$$E = \langle E(\text{receptor}) + E(\text{ligand}) - E(\text{receptor} + \text{ligand}) \rangle \quad \text{(Eq. 1)}$$

where E(receptor) = potential energy of siglec-1; E(ligand) = potential energy of Neu5Ac, Neu5Gc, Neu5Prop, or Neu5But, respectively; E(receptor + ligand) = potential energy of the complex; $\langle\ \rangle$ means averaging over all snapshots.

The solvation energy was calculated using the boundary element method implemented in YASARA (29). The boundary between solvent (dielectric constant 78) and solute (dielectric constant 1) was formed by the latter's molecular surface, constructed with a solvent probe radius of 1.4 Å, and the following radii for the solute elements: polar hydrogens 0.32 Å; other hydrogens 1.017 Å; carbon 1.8 Å; oxygen 1.344 Å; nitrogen 1.14 Å; sulfur 2.0 Å. The solute charges were assigned based on the AMBER03 force field (32), using GAFF/AM1BCC (35) for the ligands.

Docking and Post-scoring—The receptor was prepared for docking using LeadIT 2.1.7 (BioSolveIT GmbH, Sankt Augustin, Germany) based on the crystal structure of mouse Siglec-1 (PDB code 1OD7). Neu5Ac, Neu5Gc, Neu5Prop, and Neu5But were minimized using YASARA (29) and docked using FlexX

(37). Ten poses were generated for each ligand and scored using SeeSAR (BioSolveIT GmbH, Sankt Augustin, Germany), which uses the HYDE scoring function (38).

Analysis of Modified Sialic Acids—Concentrations of total membrane-bound and glycolipid-bound sialic acids were measured by DMB-HPLC (39). Approximately 100,000 293T cells were cultured in DMEM (10% FBS, 2 mM L-glutamine, 2 mM sodium pyruvate) containing ManNAc or its analogs (5 mM ManNAc, 5 mM ManNProp, 5 mM ManNCyclo, 5 mM ManNBut, 0.3 mM Ac_4ManNAc, or 0.3 mM Ac_4ManNGc). The medium was renewed on day 5. After 7 days the cells were harvested and homogenized by sonication in ice-cold lysis buffer (150 mM NaCl, 10 mM Tris, 5 mM EDTA, 1 mM PMSF, 40 μM leupeptin, 1.5 μM aprotinin, pH 8.0) (40). A stepwise chloroform/methanol precipitation was performed on half of each sample to extract the glycolipid fractions (41). Membrane fractions were isolated from the remaining cell lysates by centrifugation at 21,000 × *g* and 4 °C for 2 h. Protein concentrations in the supernatants (representing the cytosolic compartment) were measured using the bicinchoninic acid assay (BCA, Pierce). All membrane and glycolipid fractions were hydrolyzed with 1 M trifluoroacetic acid (TFA) for 4 h at 80 °C, as described previously (42). Hydrolyzed samples were dried and subsequently dissolved in 5 μl of TFA (120 mM). Samples were labeled for 2 h at 56 °C with 30 μl of DMB solution (6.9 mM DMB, 0.67 mM β-mercaptoethanol, 0.19% sodium bisulfite).

Labeled samples were analyzed on an Agilent 1200 HPLC system using a Gemini-NX C18 column (110 Å, 3 μm particle size, 4.6 × 150 mm, Phenomenex). Probes were separated at 0.5 ml/min flow rate with methanol/acetonitrile/water (6:8:86) as eluent. The detector was configured with 373 nm for excitation and 448 nm for emission. To quantify the occurring sialic acid species, DMB-labeled standards were injected: Neu5Ac (Sigma), Neu5Gc (a gift from R. Schauer, University of Kiel), and Neu5But (a gift from C. R. Bertozzi, Stanford University). Concentrations of Neu5Prop and Neu5Cyclo were estimated according to the Neu5Ac standard. Unlabeled standards and HPLC retention peaks of interest were further analyzed by LC-electrospray-ionization mass spectrometry (ESI-MS). Therefore, 20 μl of collected sample or 500 ng of the respected standard dissolved in H_2O were injected into an Agilent 1100 series LC/MSD system with 79.9% methanol, 20% isopropyl alcohol, and 0.1% formic acid as eluent, 0.5 ml/min flow rate, 4 kV capillary voltage, and 350 °C capillary temperature.

Statistical Analyses—Plotting of graphs and general statistical analyses were performed using the GraphPad Prism 5 software package (GraphPad Software Inc., La Jolla, CA). This software was also used to calculate Pearson correlation coefficients and significance values by applying the two-tailed, unpaired Student's *t* test.

Results

Mouse Siglec-1 Is Expressed on Macrophages, Up-regulated by IFNα, and Mediates MLV trans-Infection of Lymphocytes—To explore the expression of Siglec-1 on the cell surface of mouse macrophages, macrophage cell line ANA-1 and primary BMDM were stained with either rat anti-mouse Siglec-1 mAb 3D6.112 or an isotype control mAb and processed for flow

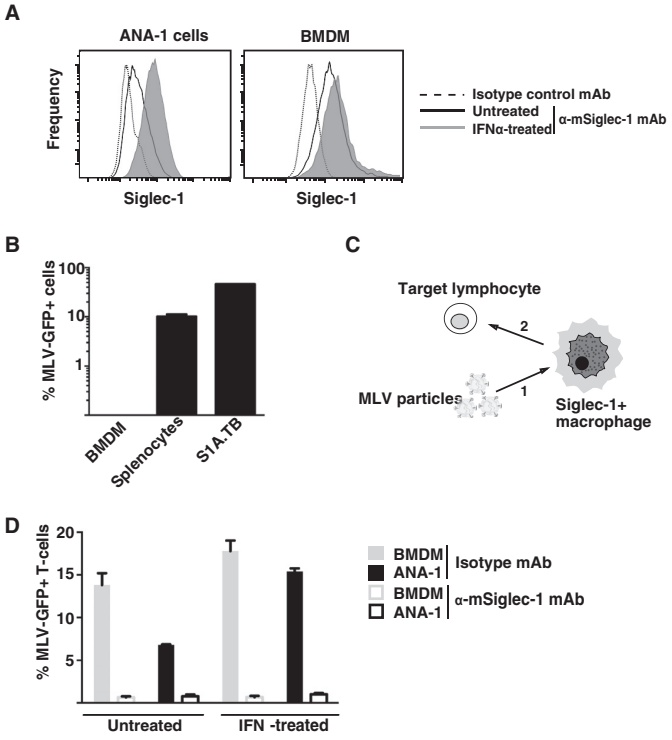

FIGURE 1. **Siglec-1 is expressed on mouse macrophages in an IFNα-responsive manner and supports MLV *trans*-infection.** *A,* ANA-1 cells or BMDM were stimulated with mouse IFNα (500 units/ml) for 48 h or left untreated. Mechanically detached cells were stained using a phycoerythrin-conjugated anti-mSiglec-1 mAb or an isotype control mAb and analyzed by flow cytometry. Shown are untreated cells (*black lines*) or IFNα-treated cells (*shaded histograms*) stained for mSiglec-1 and untreated cells (*dotted line*) stained with the isotype mAb. *B,* each of the indicated cell types was infected with MLV-GFP (m.o.i. 0.1) and 2 days later analyzed for GFP expression, indicative of productive infection, by flow cytometry. *C,* experimental setup for assessment of MLV *trans*-infection. *1,* addition of MLV particles to macrophages; *2,* addition of target lymphocytes to macrophage culture. *D,* BMDM or ANA-1 cells were stimulated with mouse IFNα (500 units/ml) for 48 h or left untreated. Cells were preincubated with an anti-Siglec-1 mAb or an isotype control mAb at 4 °C, exposed to MLV-GFP (m.o.i. 0.1) for 4 h at 37 °C, and washed three times in PBS. S1A.TB cells were then added in a 1:1 ratio to the virus-pulsed macrophage cultures for 48 h and then analyzed for GFP expression by flow cytometry. Data are expressed as the arithmetic means ± S.D. of triplicate samples from one mouse and are representative of at least two experiments each performed using 2–3 mice.

cytometry. Cells that had either been left untreated or exposed to mouse IFNα for 48 h were analyzed. ANA-1 cells expressed low constitutive levels of Siglec-1 on the surface, the expression of which could be induced 3-fold by IFNα stimulation (Fig. 1*A*). BMDM expressed markedly higher constitutive levels but also INFα-responsive levels of the sialic acid-binding Ig-like receptor on their cell surface (Fig. 1*A*).

For studies on direct infection or *trans*-infection, we employed a replication-competent ecotropic Moloney MLV carrying an IRES-*egfp* element (MLV-GFP) (67) that had been produced in human 293T cells. The GFP reporter encoded by this recombinant retrovirus is expressed only upon productive infection of target cells. We first characterized the susceptibility of the cell lines and primary cells used in this study for direct, productive MLV-GFP infection. Virus exposure of the S1A.TB.4.8.2 (S1A.TB) T-cell lymphoma or LPS-activated primary mouse splenocytes demonstrated their high level susceptibility, although BMDM were non-permissive (Fig. 1*B*). The

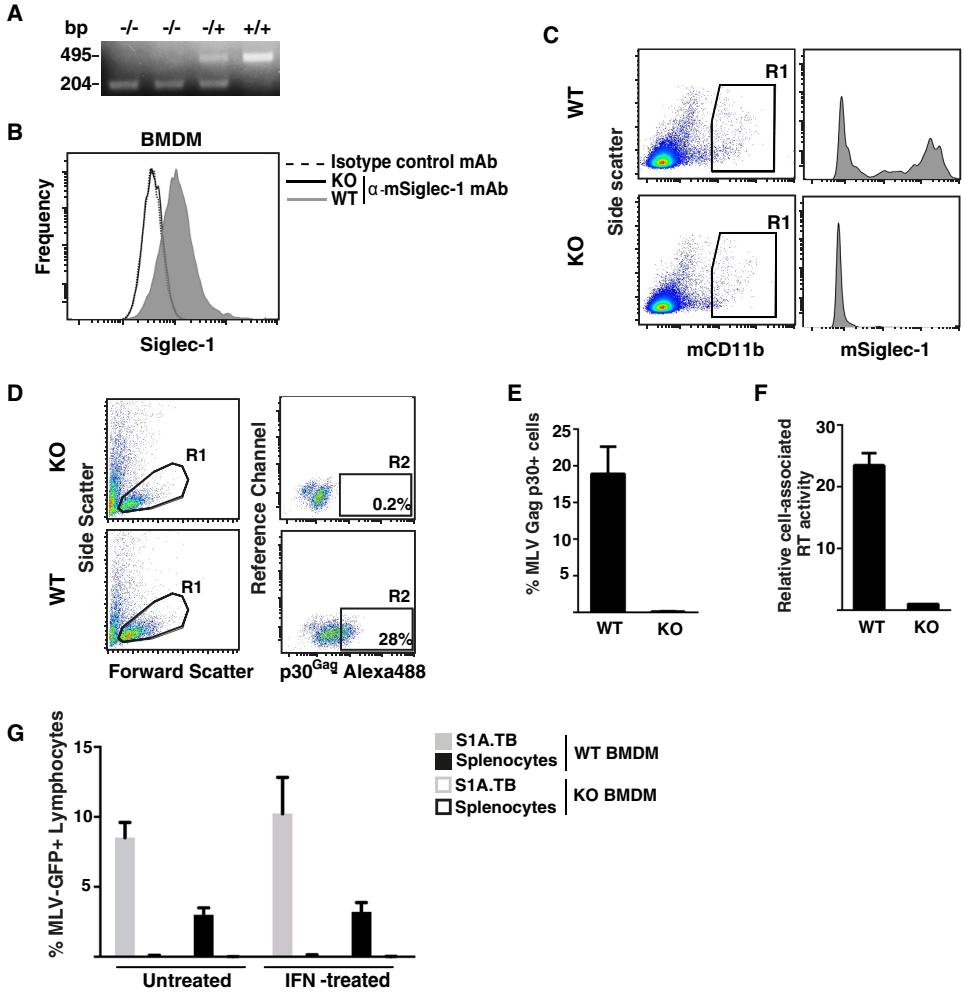

FIGURE 2. **BMDM from WT, but not from Siglec-1KO mice, support MLV capture and *trans*-infection.** *A,* genotyping of KO and heterozygous mice by PCR. DNA extracted from mouse tails was amplified using an allele-specific PCR. Product sizes of 495 or 204 bp are diagnostic for the WT and KO allele, respectively. *B* and *C,* Siglec-1 phenotyping of KO and WT mice. L929-differentiated BMDM (*B*) or freshly isolated, mechanically disrupted inguinal lymph nodes (*C*) were stained for mSiglec-1 surface expression (in *C,* co-stained for mCD11b) and analyzed by flow cytometry. *B,* shown are WT-BMDM (*shaded histogram*) or KO-BMDM (*black line*) stained for mSiglec-1 and WT-BMDM (*dotted line*) stained with the isotype mAb. *D–G,* BMDM from WT and KO mice were exposed to MLV-GFP for 4 h at 37 °C and subsequently washed three times with PBS. *D* and *F,* MLV-GFP-pulsed BMDM were detached and analyzed for MLV capture by two methods. *D* and *E,* first, pulsed cells (m.o.i. 0.5) were fixed, permeabilized, and stained with rat anti-$p30^{Gag}$ mAb followed by an Alexa488-conjugated secondary antibody. *D,* dot plots from flow cytometric analyses depicting (*left panels*) the forward and side scattering of light to identify live cells (gate *R1*) and (*right panels*) Alexa488 staining to identify cell-associated MLV $p30^{Gag}$ (gate *R2*) are shown. The percentage of viable, $p30^{Gag}$ + cells within R2 is indicated. *E, chart bars* depict the arithmetic means ± S.D. of the percentage of $p30^{Gag}$-positive cells from triplicates. *F,* second, pulsed cells (m.o.i. 0.1) were detached, lysed, and analyzed for cell-associated RT activity. *G,* MLV-GFP-pulsed BMDM were co-cultivated with LPS-activated splenocytes or S1A.TB cells at a 1:1 ratio. 48 h later, lymphocytes were analyzed for GFP expression by flow cytometry. Data are expressed as the arithmetic means ± S.D. of triplicate samples from one KO and one WT mouse and are representative of at least two experiments each performed using 2–3 mice.

inability of MLV to infect non-cycling macrophages is well established (43, 44) and an important characteristic to unambiguously assess their role as a virus donor in MLV *trans*-infection of lymphocytes in this study.

To explore the ability of mouse macrophages to capture and *trans*-infect target cells with MLV-GFP in a Siglec-1-dependent manner, BMDM or ANA-1 cells were first pretreated for 30 min at 4 °C with blocking anti-Siglec-1 or isotype control mAbs, then exposed to MLV-GFP particles for 4 h at 37 °C, washed extensively, and subsequently co-cultured with target S1A.TB lymphoma cells (Fig. 1*C*). Two days later, the percentage of GFP-positive S1A.TB cells was analyzed by flow cytometry as a quantitative readout for the efficiency of *trans*-infection. ANA-1 cells and BMDM, which had been pretreated with an isotype control mAb, mediated a robust MLV-GFP *trans*-infection (Fig. 1*D*). Their capacity for *trans*-infection was increased by IFNα pretreatment (Fig. 1*D*), and this effect largely correlated with their Siglec-1 surface levels (Fig. 1*A* and data not shown). Importantly, MLV *trans*-infection was efficiently and specifically blocked when macrophages were pretreated with the anti-mouse Siglec-1 mAb 3D6.112 (Fig. 1*D*). Thus, Siglec-1 on the cell surface of BMDM is constitutively expressed, IFNα-responsive, and has the capacity to mediate *trans*-infection of the retroviral pathogen MLV to permissive lymphocytes.

BMDM from Wild-type, but Not from Siglec-1 KO Mice, Support MLV Capture and trans-Infection—To further corroborate the role of mSiglec-1 in MLV *trans*-infection, we employed Siglec-1 KO mice (8). The genotype of mice was determined using an allele-specific PCR (Fig. 2*A*). The absence of Siglec-1 expression in KO mice carrying the homozygous(−/−) dele-

tion was demonstrated in cultured BMDM (Fig. 2*B*) and mCD11b-positive cells of the monocyte/macrophage lineage in a freshly isolated lymph node suspension (Fig. 2*C*), in line with previous characterizations (45).

In a comparative assessment of Siglec-1 KO and wild-type (+/+, WT) mice, we quantified Siglec-1-dependent capture of MLV particles by BMDM. Two experimental approaches were taken; BMDM from WT and KO mice were incubated with MLV for 4 h at 37 °C, washed with PBS, detached by gentle scraping, and processed for detection of either cell-associated MLV $p30^{Gag}$ structural protein or cell-associated reverse transcriptase (RT) activity. For the first approach, BMDM were fixed, permeabilized, and stained using a rat anti-$p30^{Gag}$ mAb. Although flow cytometric analysis of MLV-exposed KO-BMDM showed only background staining (Fig. 2, *D*, *upper panel* (gate *R2*), and *E*), BMDM from WT littermates revealed a robust signal for the $p30^{Gag}$ capsid staining (Fig. 2, *D*, *lower panel* (gate *R2*), and *E*).

For the second approach, BMDM were lysed and processed for a SYBR Green I-based product-enhanced RT assay, a method previously developed for the quantitation of retroviruses in culture supernatants (31, 46). MLV exposure of WT-BMDM, but not of KO-BMDM, resulted in a significant cell-associated RT activity (Fig. 2*F*).

Next, BMDM derived from WT and KO mice were analyzed side-by-side for their capacity to mediate MLV *trans*-infection. In line with the above antibody-blocking studies (Fig. 1*D*), WT-BMDM efficiently *trans*-infected S1A.TB T-lymphocytes and LPS-stimulated splenocytes (Fig. 2*G*). In contrast, KO-BMDM were unable to support MLV *trans*-infection, and IFNα stimulation could not overcome this limitation (Fig. 2*G*). Together, these results demonstrate that primary macrophages from mice are capable of capturing infectious MLV particles and of mediating a subsequent *trans*-infection of lymphocytes in a Siglec-1-dependent manner.

MLV-GFP trans-Infection Is an Efficient Process That Preferentially Targets Primary Activated B-cells—Next, we sought to assess the relative contribution of direct infection as compared with *trans*-infection to the overall infection of cultured primary lymphocytes in the context of a constant multiplicity of infection. Moreover, we tested the impact of two activation protocols for splenocyte cultures, *i.e.* treatment with either LPS or ConA/IL-2, which preferentially stimulate the proliferation of B-cells and T-cells, respectively (47, 48), on the MLV-GFP susceptibility of lymphocytes under these conditions.

WT splenocyte cultures following LPS activation for 3 days consisted of 64% CD19-positive and 31% CD3-positive cells, expressed as fractions within the viable lymphocyte gate (Fig. 3*A*, *left lower panel*). In contrast, stimulation with ConA/IL-2 resulted in 97% CD3-positive T-cells (Fig. 3*B*, *left lower panel*). Two interesting observations were made. First, in the absence of BMDM ("splenocytes only"), only LPS stimulation allowed for a robust direct infection of WT splenocytes (4.0 ± 0.8%, Fig. 3*C*), the vast majority of which were blasted CD19-positive B-cells (99.8%, data not shown). In comparison, the low level infection of the ConA/IL-2-stimulated culture (0.2 ± 0.08%, Fig. 3*C*) represented both T-cells (63%) and B-cells (24%) (data not shown). Second, the experimental setup, in which WT splenocytes (targets for both direct and *trans*-infection) and

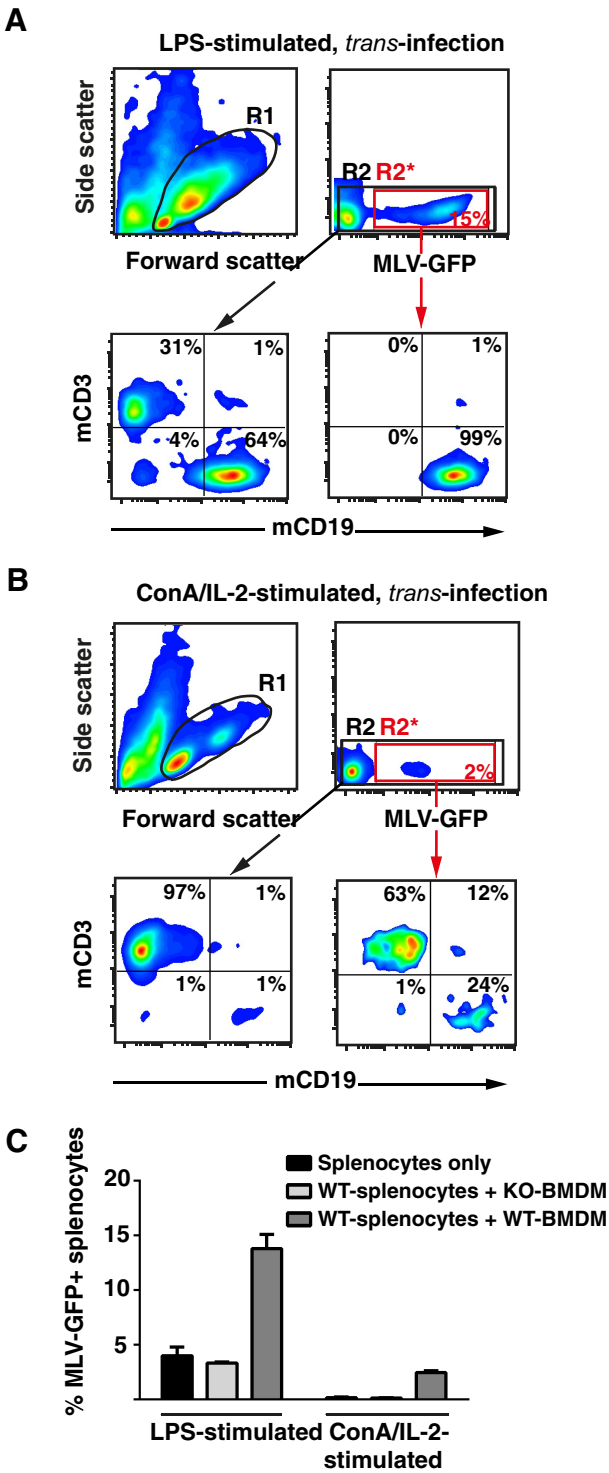

FIGURE 3. **BMDM-mediated *trans*-infection of MLV-GFP efficiently targets activated primary B-cells.** Splenocytes from WT mice were activated with either LPS (*A*) or ConA/IL-2 (*B*) for 3 days and then seeded either alone or onto BMDM from WT or KO mice in a ratio of 1:1. Cultures were challenged with MLV-GFP (m.o.i. 0.2) and splenocytes analyzed for GFP expression 48 h later by flow cytometry. *A* and *B*, effect of activation protocols, and the identity of MLV-GFP-infected splenocytes was determined by co-staining for the lineage markers CD3 (T-cells) and CD19 (B-cells). *R1* identifies the viable cells. *R2** (*red box*) identifies the MLV-GFP-positive cells and *R2* (*black box*) all viable cells. Dots plots in the *lower panels* depict the respective mCD3/mCD19 stainings. *C*, *chart bars* depict the arithmetic means ± S.D. of the percentage of GFP-positive, viable cells from analyses performed in triplicate. Experiments were performed using 2–3 KO or WT mice and were repeated at least twice showing similar results.

BMDM (donor cells for *trans*-infection) were present in the culture at the time of virus addition, revealed that WT-BMDM, but not KO-BMDM, were able to markedly boost the overall infection level of lymphocytes, respectively (Fig. 3*C*). For LPS-stimulated splenocytes, the co-culture with WT-BMDM raised the percentage of GFP-positive lymphocytes to 14.0 ± 1.3%, representing a 3–5-fold increase over the conditions with splenocytes alone or co-culture with Siglec-1-deficient BMDM (Fig. 3*C*). Virtually all infected cells were CD19-positive B-cells (Fig. 3*A*, *lower right panel*). Remarkably, co-culture with WT-BMDM resulted also in a notable infection of ConA/IL-2-activated splenocytes translating to a 15-fold enhancement over the reference conditions (Fig. 3*C*) with both T-cells and B-cells being infected (Fig. 3*B*). Collectively, these results indicate that Siglec-1-dependent *trans*-infection via macrophages may contribute to a more efficient infection process of lymphocytes in the context of a limited number of infectious MLV particles. Moreover, activated primary B-cells appear to be a preferential target of direct infection as well as *trans*-infection of MLV.

Mouse Siglec-1 and MLV Gag Partially Co-localize Early after Virus Exposure—Next, we investigated the fate of Siglec-1 and MLV in BMDM early and late after virus exposure by co-immunofluorescence microscopy and *trans*-infection analysis. BMDM derived from WT or KO mice were pulsed with either MLV-GFP or MLV-Gag-GFP for 4 h at 37 °C and then extensively washed. The latter virus carries Gag-GFP fusion proteins within the particle.

BMDM cultured on coverslips were either fixed immediately after pulse ("4 h") or cultivated for another 20 h ("24 h") and stained with antibodies to mSiglec-1. At the 4-h time point, mSiglec-1 and Gag-GFP partially co-localized in distinct punctae in WT-BMDM (Fig. 4*A*, *upper* and *middle panels*). Here, two phenotypes were frequently observed. A dominant single accumulation of the mSiglec-1 receptor and the viral structural protein was observed in 69% of cells (Fig. 4, *A* (*upper panels*) and *B*), resembling the sac-like compartment reported for human Siglec-1 and HIV $p24^{Gag}$ in myeloid dendritic cells (1, 34). In 31% of BMDM, a more scattered cytoplasmic localization of Siglec-1 and Gag-GFP was noted with up to 100 distinct punctae, in which signals for both proteins partially overlapped (Fig. 4, *A* (*middle panels*) and *B*). No co-localization of the mSiglec-1/Gag-GFP-positive punctae with a marker for acidic lysosomes was observed (data not shown). BMDM from KO mice displayed only background staining for mSiglec-1 and at most a few small Gag-GFP signals (Fig. 4*A* (*lower panels*)). Interestingly, at 24 h, the frequency and intensity of the punctae for both mSiglec-1 and Gag-GFP in WT-BMDM were strongly diminished (Fig. 4*C*).

In parallel to the microscopic analyses, we assessed the ability of BMDM to *trans*-infect S1A.TB cells immediately after the virus pulse (4 h) and after the prolonged storage period of 24 h. Remarkably, delayed addition of target T-cells at only 24 h resulted in a drastic drop in the efficiency of *trans*-infection, levels of 2% compared with the condition in which the S1A.TB cells had been added to the BMDM at the 4-h time point (Fig. 4*D*). Similarly, levels of cell-associated RT activity were also found to be drastically decreased at the 24-h time point (Fig. 4*E*). Of note, neither the loss of capsid signal in immunofluorescence nor the drop in *trans*-infection could be rescued by pretreating the BMDM with proteasomal or lysosomal inhibitors at non-toxic concentrations (data not shown). In conclusion, mSiglec-1 and MLV Gag partially co-localize in BMDM early after virus exposure. Within 24 h, the detection of the viral structural protein is greatly diminished coinciding with a marked reduction in the ability of pulsed BMDM to *trans*-infect.

Mainly Surface-bound MLV Particles trans-Infect Lymphocytes—To investigate whether the MLV particles responsible for *trans*-infection are internalized into BMDM or are still accessible at the cell surface, we used short term proteolytic digestion to remove surface-bound particles after virus pulse. We found that BMDM that had been treated with Pronase, a protease mixture that digests extracellular proteins, including viral proteins, transferred considerably less MLV particles than untreated BMDMs (Fig. 4*F*). The reduction was dependent on the Pronase concentration, while BMDM viability was not affected. As controls of specificity, boiled Pronase had no effect on *trans*-infection (Fig. 4*F*), and supernatants from Pronase-treated and subsequently washed BMDMs, which had not been exposed to MLV, did not affect the ability of MLV-GFP for direct infection of target lymphocytes (Fig. 4*G*). Collectively, these results indicate that MLV particles that are captured by Siglec-1-positive macrophages and that are responsible for *trans*-infection remain surface-bound and are not internalized into a strictly "intracellular" compartment in BMDM.

Detection of Biosynthetically Modified Sialic Acids in Glycolipids and Glycoproteins in Cells Pretreated with N-Acyl-modified D-Mannosamines—We then sought to functionally explore the role of sialic acid for the Siglec-1-dependent *trans*-infection of MLV at a submolecular level in living cells by employing metabolic glycoengineering (23, 49). This experimental approach is based on the established ability of synthetic *N*-substituted D-mannosamine (ManN) derivatives to act as metabolic precursors for sialic acids with structurally altered *N*-acyl side chains incorporated into cellular glycoconjugates, including sialylated gangliosides that are incorporated into budding retroviruses (50, 51).

We first pretreated 293T cells with six different synthetic *N*-acyl-modified ManN analogs (Fig. 5*A*) or the most common physiological precursor, *N*-acetyl ManN (ManNAc), for 5 days at non-toxic concentrations. For two analogs (ManNProp and ManNGc) and ManNAc also, peracetylated (Ac4) derivatives were used, which facilitate the cellular uptake of the compounds and therefore require considerably lower concentrations for treatment. Subsequently, re-seeded cells were transfected with MLV-GFP proviral DNA and cultivated in the presence of the respective ManN derivatives for 2 more days. Released MLV-GFP particles were concentrated and purified by ultracentrifugation through a sucrose cushion.

As quality controls for analysis, ESI-MS was used to determine the purity of the sialic acid standards (Fig. 5*B*), and the presence of the DMB-labeled sialic acid species was verified in the collected retention peaks (Fig. 5*C*). Chromatograms of glycolipid-bound (Fig. 6*A*) and total membrane-bound (data not shown) sialic acids were used to quantify their respective concentrations. Alterations of the sialylation pattern of the cells

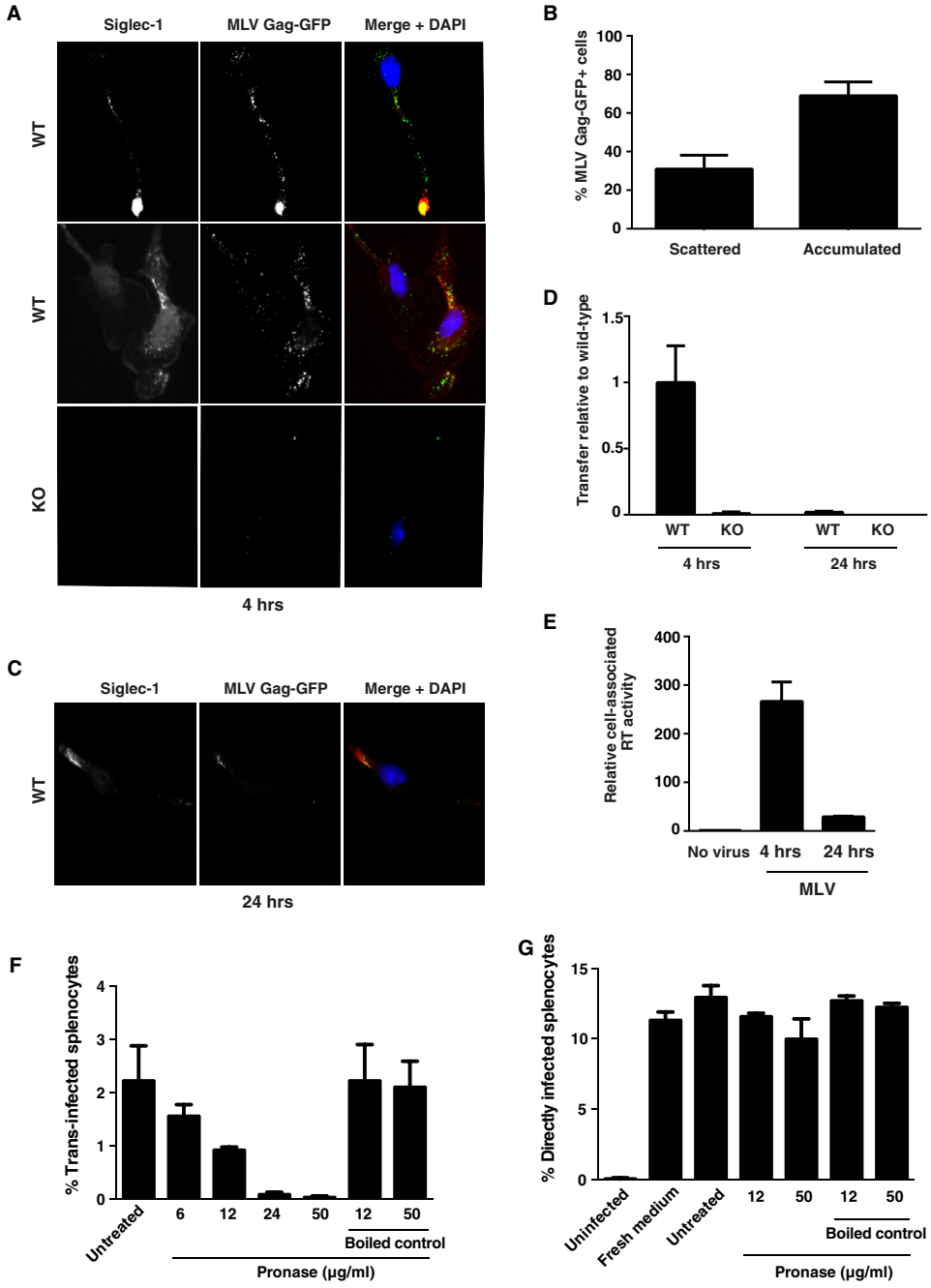

FIGURE 4. **Captured MLV particles partially co-localize with Siglec-1 in BMDM early after virus exposure, and surface-bound MLV is the primary source for *trans*-infection.** BMDM derived from either WT or KO mice were pulsed with MLV Gag-GFP, which carries a Gag-GFP fusion protein (*A–C*), or MLV-GFP, for 4 h at 37 °C (*D* and *E*). PBS-washed BMDM were either co-cultivated with S1A.TB-cells added either immediately after washing (4 h) or 20 h later (24 h) (*D*) or fixed, permeabilized, and stained using an Alexa647-conjugated anti-Siglec-1 mAb (*A–C*). Representative images for a dominant single accumulated MLV Gag/Siglec-1 signal (*A, upper panels, 4 h*) or multiple scattered punctae from WT-BMDM (*A, middle panels, 4 h*) are shown. *A, bottom panel,* images of MLV-Gag-GFP-pulsed KO-BMDM stained for mSiglec-1. *B,* MLV Gag pattern ("scattered" or "accumulated") and frequency of WT-BMDM displaying this phenotype were quantified. At least 70 cells from each of three mice were analyzed. *E,* cell-associated RT activity was quantified using SG-PERT, and values are depicted as activity associated with WT cells relative to KO cells. *F* and *G,* BMDM were pulsed with MLV-GFP for 4 h at 37 °C. PBS-washed BMDM were treated with increasing concentrations of cleavage-competent active Pronase for 30 min at 4 °C. After Pronase inactivation through washes in FBS-containing medium, cells were co-cultured with LPS-activated splenocytes for assessment of *trans*-infection. *F,* BMDM, in the absence of MLV, were treated as in *G*, then washed with PBS, and cultivated for 1 h more at 37 °C. These culture supernatants were then mixed with MLV-GFP to assess their potential impact on *direct* MLV-GFP infection of splenocytes.

were noted for all treatment conditions, both in the total membrane fraction (glycoproteins and glycolipids) and in the glycolipid fraction alone (Fig. 6, *A* and *B*). Growth of 293T cells in the presence of either synthetic ManNProp, ManNCyclo, ManNBut, or AcManNGc resulted in the detection of unnatural sialic acid carrying the corresponding *N*-acyl substitution. Both the overall concentration of *N*-acyl-modified sialic acids (Fig. 6*B*) and their abundance relative to Neu5Ac varied considerably; Neu5But represented 23% of all sialic acids in the total membrane fraction and 48% in the glycolipid fraction of ManNBut-

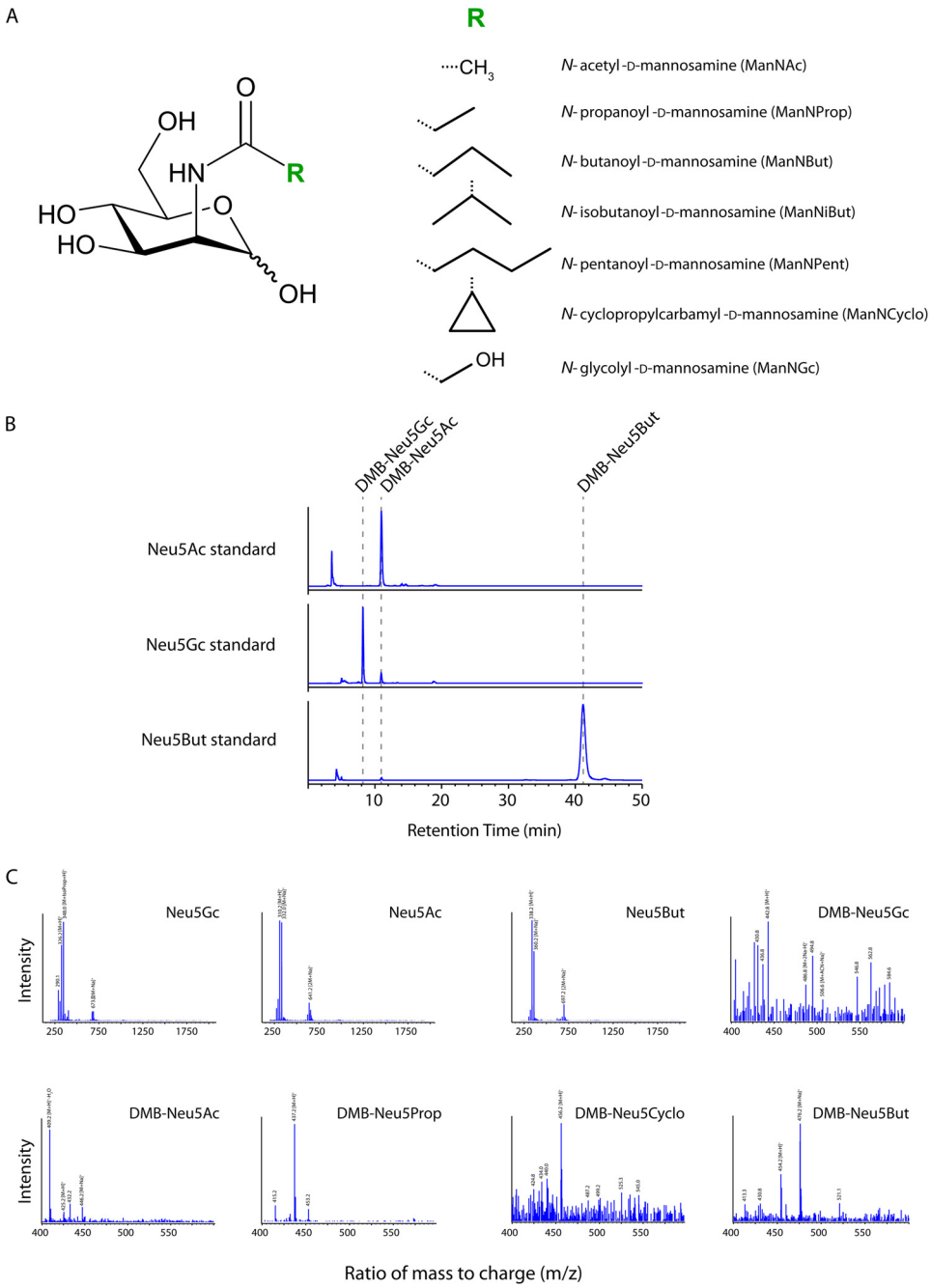

FIGURE 5. **Biosynthetic modification of the of *N*-acyl side chain of sialic acids in glycoconjugates of ManN analog-treated virus producer cells.** *A,* schematic representation of ManNAc and the applied *N*-substituted ManNs with *R* indicating the modified *N*-acyl group. *B,* representative chromatograms of DMB-labeled sialic acid standards. Retention times (*dashed lines*) and peak areas of the sialic acid standards were determined after injecting 30 ng of the respected DMB-labeled species into the HPLC system. *C,* mass spectra of standards and DMB-labeled sialic acid species found in the lysates of 293T cells treated with different ManN derivatives. HPLC retention peaks were collected and subsequently analyzed by ESI-MS. 20 μl of the collected retentions peaks or 500 ng of the respected standard dissolved in H_2O were injected into the LC-MSD system. DMB labeling of sialic acids leads to an increase in the molecular mass of 116.2 Da. Masses of the different sialic acid species are depicted, partly with common adducts. *ACN*, acetonitrile; *IsoProp*, isopropyl alcohol.

treated cells. In ManNProp-treated cells, Neu5Prop comprised 76% of the detected sialic acids in the total membrane fraction and 83% in the glycolipid fraction. Representing the most drastic change in sialic acid composition, 91 or 93% of all sialic acids in ManNCyclo-pretreated cells were identified to be Neu5Cyclo in the total membrane or glycolipid fraction, respectively (Fig. 6, *A* and *B*). Overall, there was a trend toward a higher abundance of biosynthetically modified sialic acids in the glycolipid fraction alone as compared with the total membrane fraction. As a side note, small amounts of Neu5Gc, which is normally not found in human cells (52), were also detected in some of the cells that had not been pretreated with synthetic Ac_4ManNGc (Fig. 6, *A* and *B*). This most likely occurred through a salvage pathway that recruits Neu5Gc from fetal bovine serum sialoglycoconjugates in the media (53). Thus, addition of D-ManN analogs carrying *N*-acyl substitutions to cultured 293T cells for several days prior to their use as MLV producer cells resulted in the bio-

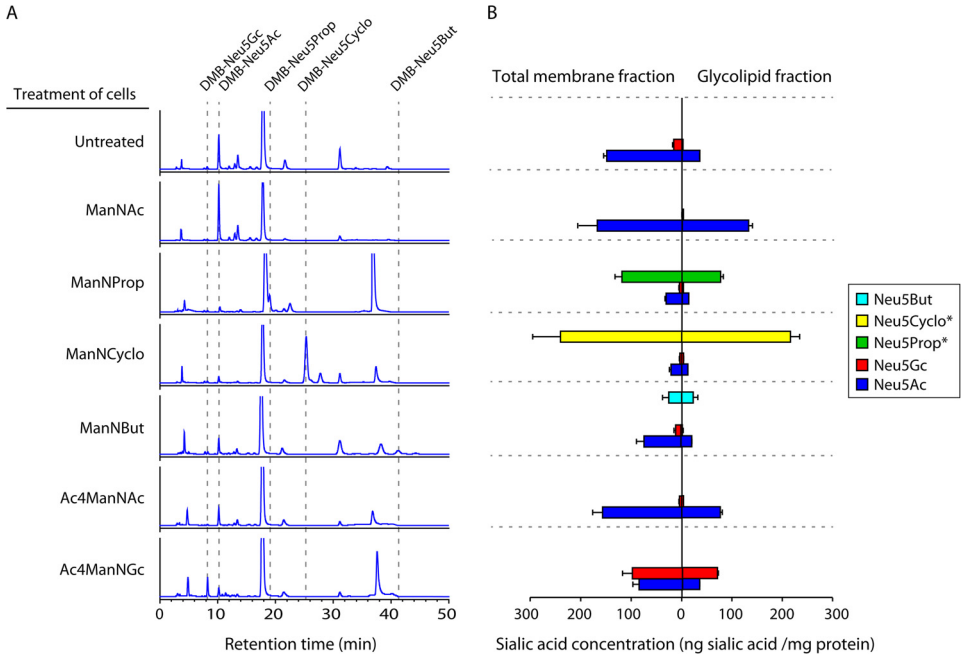

FIGURE 6. **High level detection of biosynthetically modified sialic acids in glycoconjugates of *N*-acyl-modified ManN-treated virus producer cells.** *A* and *B,* characterization and quantification of glycolipid-bound sialic acids by DMB-HPLC. 293T cells were treated for 7 days with the respective ManN derivatives. A medium change was performed on day 5. To calculate the concentrations of the occurring sialic acid species, retention peak areas of interest were compared with the retention peak areas of standards (Fig. 5*C* and data not shown) and normalized to the cytosolic protein concentrations of the respective cell lysates. Internal standards were used for Neu5Ac, Neu5Gc, and Neu5But (Fig. 5*B*). Concentrations of Neu5Prop and Neu5Cyclo were estimated according to the Neu5Ac standard (*). *B,* data shown represent the mean values and S.D. of two independent experiments ($n = 2$).

synthetic incorporation of up to 93% of unnatural sialic acid in cellular glycoconjugates.

Biosynthetic Modulation of the N-Acyl Side Chain of Sialic Acid in Virus Producer Cells Affects the Ability of Released MLV Particles for Siglec-1-dependent Capture and trans-Infection—The preparations of MLV-GFP particles released from ManN analog-pretreated 293T cells were first titered on S1A.TB T-cells, the binding and infection process of which is mediated by the mCAT-1 receptor in a sialic acid-independent manner (54).

Employing our standard experimental setup, these MLV-GFP particle preparations were assessed for their functionality to be captured by Siglec-1-positive WT-BMDM and to *trans*-infect S1A.TB T-cells. In parallel, the inocula of the different MLV-GFP stocks were used to infect S1A.TB T-cells directly (Fig. 7*A*), confirming that comparable infectious titers had indeed been applied.

Striking functional differences were, however, observed for virus capture by BMDM and *trans*-infection. First, MLV-GFP particles released from 293T cells pretreated with *N*-butanoyl, *N*-isobutanoyl, *N*-glycolyl, or *N*-pentanoyl-modified sialic acid precursor analogs were only inefficiently captured by BMDM, whereas ManNProp or ManNCyclo treatments had no or only slight effects (Fig. 7, *B–D*). Levels of cell-associated MLV $p30^{Gag}$ staining and cell-associated RT activity were reduced by up to 92% (Fig. 7, *B* and *C*) and these readouts for virus capture strongly correlated with each other (Fig. 7*E*, $r = 0.91$, $p = 0.0008$).

Second, in support of a cardinal role of virus capture for the efficiency of subsequent *trans*-infection, levels of MLV-GFP infection in S1A.TB cells were markedly reduced for viruses derived from producer cells exposed to the *N*-butanoyl, *N*-isobutanoyl, *N*-glycolyl, or *N*-pentanoyl ManNs (Fig. 7*D*), and these infection levels correlated with both readouts for virus capture (Fig. 7, *F* and *G*).

Taken together, these results indicate that biosynthetic engineering of glycoconjugates in virus-producer cells is a feasible strategy to alter the composition of sialylated glycolipids and glycoproteins within the envelope of viruses that bud from the plasma membrane allowing their functional characterization. Specifically, this approach allowed us to identify the *N*-acyl side chain of sialic acid as a critical determinant for the interaction of MLV particles with mSiglec-1 in a native environment.

Molecular Modeling of Siglec-1 in Complex with Sialic Acid Derivatives Suggests Altered Interaction Affinities for Specific N-Acyl Side Chain Modifications—To further explore and possibly rationalize the impact of some of these *N*-acyl side chain modifications on the interaction with mSiglec-1, molecular modeling studies were carried out based on the crystal structure of the N terminus of the mouse receptor complexed with ME-A-9-*N*-(naphthyl-2-carbonyl)-amino-9-deoxy-Neu5Ac (PDB code 1OD7). Three-dimensional models of mSiglec-1 in complex with Neu5Ac, Neu5Gc, Neu5Prop, and Neu5But were generated. Notably, all ligands could be accommodated in the binding site without steric clashes (Fig. 8*A*).

Based on these structures two different computational methods were applied to model an influence of the *N*-acyl side chain modifications on the binding affinity. In a molecular dynamics (MD)-based approach, the relative binding strength of the ligands was estimated by calculation of the average potential interaction energy between mSiglec-1 and the respective ligand (Fig. 8*B*, *1st column*). The estimation of the binding free energy

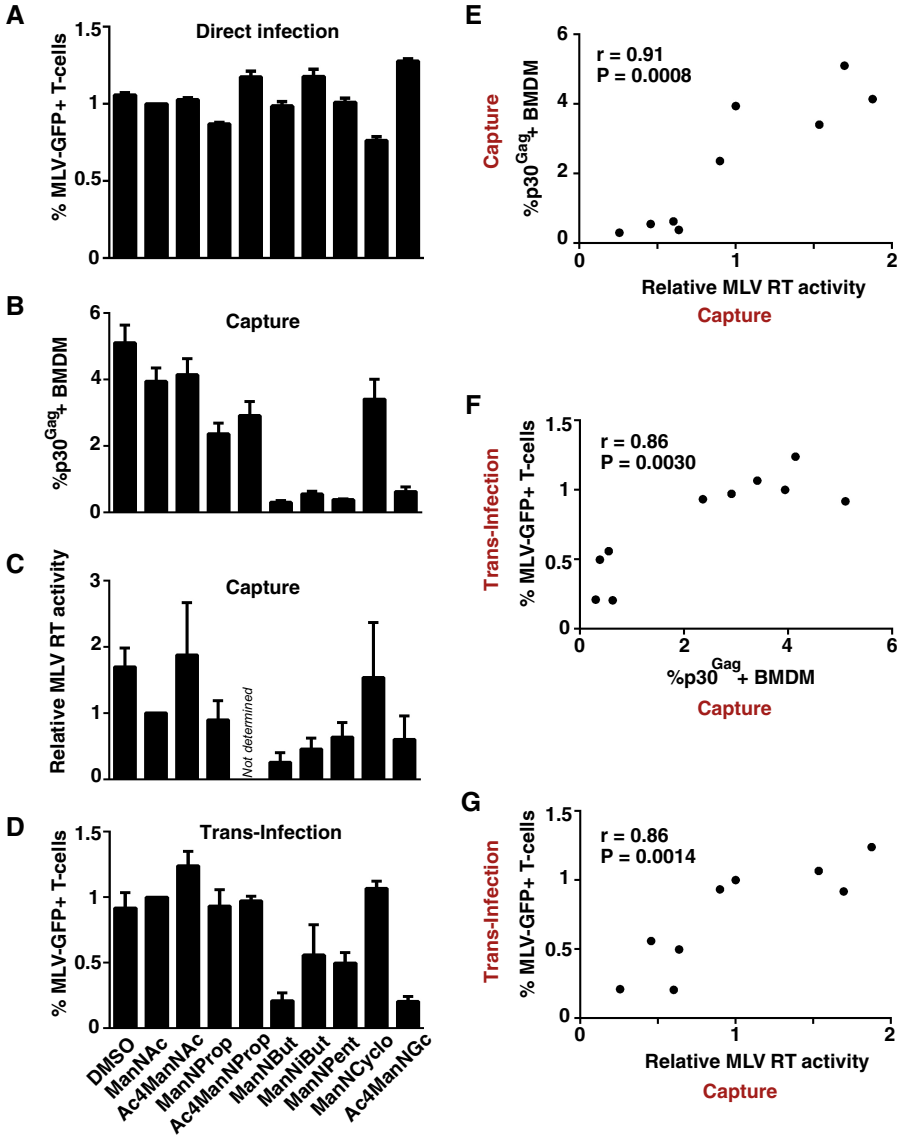

FIGURE 7. **Diminished capture and transfer of MLV particles derived from producer cells carrying specific *N*-acyl-substituted sialic acids.** *A,* S1A.TB cells were directly infected with MLV-GFP stocks (m.o.i. 0.1) produced in the absence or presence of the indicated ManN analogs and analyzed 2 days later for GFP expression. *B–D,* WT-BMDM were pulsed for 4 h at 37 °C with MLV-GFP stocks (*B,* m.o.i. 0.5; *C* and *D,* m.o.i. 0.1) produced in the absence or presence of the indicated ManN analogs. Washed cells were then either analyzed for MLV capture by quantification of $p30^{Gag}$-positive cells by flow cytometry (*B*) or cell-associated RT activity (*C*), or used for *trans*-infection of S1A.TB cells (*D*). *E–G,* correlation analysis between the relative efficiency of virus capture and *trans*-infection (data depicted in *B–D*) for the 10 different MLV-GFP stocks was performed using GraphPad Prism. Data are expressed as the arithmetic means ± S.D. of triplicate samples from one mouse and are representative of at least two experiments each performed using 2–3 mice. *r* and *p* values are shown.

from the MD data turned out to be difficult because of the significant fluctuations of the solvation free energy related to the protein (data not shown). For the isolated ligands, Neu5Gc and Neu5But, compared with Neu5Ac and Neu5Prop, had a significantly more favorable solvation energy (negative relative potential interaction energy values) indicative of a negative contribution to their binding affinity originating in the solvation.

As an alternative method to predict relative binding affinities of *N*-acyl-modified sialic acids to mSiglec-1, a "docking and post-scoring" approach was applied (for details see under "Experimental Procedures"). The values of the estimated affinity (Fig. 8*B*, *2nd column*) showed a similar trend as found in the MD-based approach, *i.e.* Neu5Gc and Neu5But were predicted to have the lowest affinity for mSiglec-1. Thus, in agreement with the functional analyses, these crystal structure-based molecular modeling studies suggest reduced binding affinities for *N*-butanoyl and *N*-glycoyl, but not for *N*-propanoyl sialic acid side chain modifications, for the interaction with mSiglec-1.

Discussion

In this study, we demonstrate that Siglec-1 is a key receptor on primary mouse macrophages for capture of the retrovirus and mouse pathogen MLV and the efficient *trans*-infection of surface-bound particles to neighboring lymphocytes. Terminal sialic acid residues on plasma membrane-derived sialyl-lactose-containing gangliosides that are incorporated into the envelope of budding retroviral particles are the key interaction moiety with the lectin receptor Siglec-1. Using metabolic glycoengi-

A

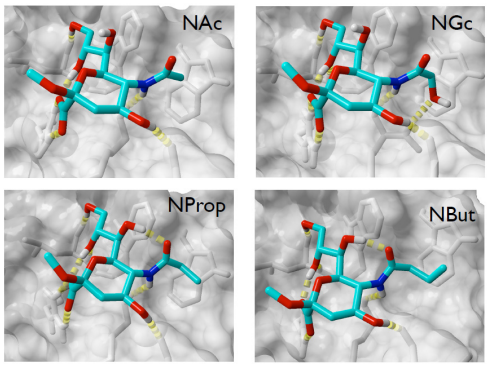

B

Relative Potential Interaction Energies and SeeSAR Affinity Scores

Ligand	Relative Potential Interaction Energy [kcal/mol]	SeeSAR Affinity Score [mM]
Neu5Ac	0	5
Neu5Prop	5.5	12
Neu5But	-6.2	26
Neu5Gc	-5.8	33

The relative average potential interaction energies were calculated from 50 ns MD simulations in water (higher values means better binding) and the average estimated affinity values calculated by SeeSAR (lower values means better binding).

FIGURE 8. **Molecular modeling of structural interaction, interaction potentials, and binding affinities of mSiglec-1 in complex with sialic acid derivatives.** *A,* three-dimensional models of mSiglec-1 in complex with Neu5Ac, Neu5Gc, Neu5Prop, or Neu5But were generated. *B,* relative potential interaction energies and SeeSAR affinity scores.

neering we introduced various *N*-acyl-modified sialic acids into glycoconjugates of virus-producer cells, and we demonstrated that for specific substitutions newly produced MLV particles were functionally impaired for Siglec-1-dependent capture and *trans*-infection. This highlights the use of sialic acid precursor analogs as a feasible approach to study the impact of submolecular modifications in glycoconjugates incorporated into enveloped viruses in a native environment and identifies the *N*-acyl side chain as a critical determinant for the mSiglec-1/MLV interaction. Collectively, mSiglec-1 is an important receptor for the sialic acid-dependent macrophage/lymphocyte *trans*-infection of MLV.

Macrophages and dendritic cells patrol peripheral mucosal sites recognizing, capturing, and processing potential pathogens into antigenic peptides for MHC class II presentation to CD4 T-cells in lymphoid tissue (55). Landmark studies proposed that HIV-1 usurps this natural DC function in the newly infected host by "hiding" inside DCs, which traffic to lymphoid organs, probably taking advantage of the formation of DC-/T-cell conjugates to promote its replication and spread (56–58). Today it is widely believed that human DCs capture and internalize infectious HIV particles into clustered "storage" compartments and subsequently transfer these virions to neighboring T-cells at virological synapses (1, 59). In contrast to the virus-promoting scenario proposed for HIV, mSiglec-1-positive sinus macrophages residing underneath the lymph node capsule were shown to act as gatekeepers at the lymph-tissue interface capturing and *trans*-presenting lymph-borne viruses, including vesicular stomatitis virus, to migrating B-cells in the underlying follicles leading to activation of effective antiviral humoral immune responses (11). Furthermore, these macrophages also appear to prevent vesicular stomatitis virus spread and fatal neuroinvasion by additional innate mechanisms (10). Of note, Siglec-1 in these studies was used as a marker for this subset of macrophages and not explored as a *bona fide* virus-binding receptor.

In contrast to the notion of an intracellular storage compartment for captured viruses that may be capable of efficient *trans*-infection of HIV-1 for up to 4 days (56, 58), Cavrois *et al.* (60) provided evidence that virions bound to the surface of monocyte-derived DCs or CD34-derived Langerhans cells, but not internalized HIV-1, was the major source of infectious virions transmitted in *trans*. This observation was recently confirmed (61). In line with these studies for HIV, our data also show that MLV particles that are still attached to the outside of BMDM, or at least accessible to protease treatment at their surface, are mainly responsible for *trans*-infection of murine lymphocytes. Moreover, we noted a marked drop of MLV *trans*-infection between the 4- and 24-h time points following virus capture by BMDM. Similarly, the HIV-1 *trans*-infection efficiency of monocyte-derived DCs was shown to be most efficient in the 1st h (60, 62). These authors also detected large amounts of internalized HIV-1 particles by confocal microscopy and suggested that this may reflect a "dead end" for functional retroviral particles. However, although neither lysosomal nor proteasomal inhibitors could prevent the apparent loss of MLV structural proteins over time in BMDM, lysosomal inhibitors did prevent the degradation of cell-associated HIV-1 in human macrophages (63).

From another perspective, given the unique subanatomical localization of Siglec-1-positive mouse macrophages in the subcapsular sinus, a "long term storage" of captured infectious virus may not at all be critical for interaction and efficient virus transmission because the preferentially targeted B-lymphocytes in the lymph follicles are closely adjacent (45). Thus, *trans*-infection of retroviruses appears to be mediated by cells of the monocytic lineage by capturing particles via surface-exposed Siglec-1. Retroviral particles that productively infect lymphocytes in *trans* originate primarily from the surface of macrophages/dendritic cells, and this process is most efficient in the 1st h following capture.

A central question for the process of *trans*-infection is its relative efficiency compared with direct infection. For HIV-1, monocyte-derived DC *trans*-infection has been suggested to be particularly effective for minimal virus doses that alone may not be sufficient for productive infection of CD4 T-cells by direct infection (56). Our results for MLV support this notion. The Siglec-1-dependent *trans*-infection of activated primary lymphocytes via BMDM, compared with direct infection, was 4–15-fold more efficient. Thus, it will be highly instructive to compare WT and Siglec-1 KO mice for the ability to support MLV replication and pathogenesis via lymphatic and intravenous challenge routes with low multiplicities of infection.

To our knowledge this study for the first time investigated the functional impact of metabolically modified sialic acids in virus producer cells on newly released viruses carrying cell-derived glycoconjugates. *N*-Substituted sialic acids could be detected and quantified in total membrane fraction and, importantly, in the glycolipid fraction of the 293T virus producer cells by DMB-HPLC and ESI-MS. More than 90% of the total cellular sialic acid content could be replaced by *N*-acyl derivatives pro-

viding a sound basis for the assessment of viruses released from these cells in sialic acid-dependent, functional assays.

Previous analyses of HIV-1 and MLV particles indicated that the overall lipid content of these retroviruses mostly matched that of the plasma membrane, with some lipids being enriched, including cholesterol, ceramide, and GM3 (50, 51). Notably, a single HIV-1 virion was estimated to contain ~12,000 sialyllactose-containing GM3 molecules that may constitute the primary interactor with the lectin receptor (1). The rather low millimolar affinity of Siglec-1 for different sialylated ligands was postulated to result in high avidity binding by receptor and ligand clustering (3). This may also be true for the interaction with viruses; HIV-1, bound initially over the entire plasma membrane, subsequently accumulated in many instances at one pole of the cell (64).

Several lines of evidence suggest that metabolically engineered gangliosides carrying *N*-acyl-modified sialic acids were indeed incorporated into MLV particles without inflicting gross structural changes to the infectious virion. First, the sialic acid-independent mCAT-mediated direct infection of lymphocytes was comparable for all MLV preparations, irrespective of the producer cell's pretreatment. In contrast, particles derived from *N*-butanoyl, *N*-isobutanoyl, *N*-glycolyl, or *N*-pentanoyl ManN-treated cells displayed strongly reduced capacities for the sialic acid-dependent mSiglec-1-mediated capture and *trans*-infection. Second, in agreement with these functional analyses, both *in vitro* interaction studies of sialylated ligands with Siglec-1 (4) and our molecular modeling studies of mSiglec-1 in complex with sialic acid derivatives indicated reduced binding affinities for the *N*-glycoyl and *N*-butanoyl, but not for the *N*-propanoyl substitution. This indicates at an atomic level that an elongation of the *N*-acyl side chain by one methyl group is still tolerated, although longer extension (Neu5But and Neu5Pent) strongly reduced the binding affinity. Interestingly, the rather bulky *N*-cyclo-propylcarbamyl side chain in glycoconjugates on MLV particles does not appear to impact the interaction with mSiglec-1, although the replacement of the methyl group (Neu5Ac) by a hydroxyl group (Neu5Gc) abolished capture and *trans*-infection.

Neu5Gc naturally occurs in mice but not in humans (65). Interestingly, it has been reported that both resting T- and B-cells preferentially carry Neu5Gc in α-2,6-linkage. Cell activation, however, results in marked changes in the glycosylation pattern, including a shift to Neu5Ac in α-2,3-linkage (36, 66). As a result, expression of Siglec-1 and Siglec-E ligands is enhanced on these lymphocytes. These changes may of course be highly relevant for MLV. On the one hand, the surface expression of selective ligands fosters the interaction of activated lymphocytes with Siglec-1-positive macrophages, increasing the likelihood for *trans*-infection. On the other hand, MLV replicates in these Neu5Ac-containing proliferating B- and T-cells, leading to the release of "Siglec-1/interaction-competent" virions.

Altogether, our study reports fundamental characteristics of *trans*-infection of the rodent pathogen MLV in primary mouse cells. We describe biosynthetic engineering of the *N*-acyl side chain of cellular sialic acid as a novel approach to study the functional impact of submolecular modifications in sialoglycans incorporated into budding enveloped retroviruses. This allowed us to identify critical determinants at atomic resolution for the Siglec-1-dependent MLV *trans*-infection in a native cellular environment.

Author Contributions—W. R. and O. T. K. conceived the study; O. T. K. and E. E. designed the experiments; E. E. performed and analyzed all MLV experiments; P. R. W., P. A., and W. R. analyzed sialic acids; M. F. performed molecular modeling analyses; I. A. assisted with mouse work; K. P., C. M., R. L. S., M. P. C., N. I.-U., and J. M.-P. provided reagents and discussion; P. R. C. provided KO mice; O. T. K. wrote the paper; and all authors commented on the manuscript.

Acknowledgments—We thank Walther Mothes for plasmids; Stephanie A. Archer-Hartmann for technical assistance; Sebenzile Myeni and Nikolas Herold for discussion; Hanna-Mari Baldauf for the coordination of animal work; and Roland Schauer and Carolyn Bertozzi for providing Neu5Gc and Neu5But, respectively.

References

1. Izquierdo-Useros, N., Lorizate, M., McLaren, P. J., Telenti, A., Kräusslich, H. G., and Martinez-Picado, J. (2014) HIV-1 capture and transmission by dendritic cells: the role of viral glycolipids and the cellular receptor Siglec-1. *PLoS Pathog.* **10,** e1004146
2. Geijtenbeek, T. B., and van Kooyk, Y. (2003) DC-SIGN: a novel HIV receptor on DCs that mediates HIV-1 transmission. *Curr. Top. Microbiol. Immunol.* **276,** 31–54
3. Crocker, P. R., Paulson, J. C., and Varki, A. (2007) Siglecs and their roles in the immune system. *Nat. Rev. Immunol.* **7,** 255–266
4. Klaas, M., and Crocker, P. R. (2012) Sialoadhesin in recognition of self and non-self. *Semin. Immunopathol.* **34,** 353–364
5. Chow, A., Huggins, M., Ahmed, J., Hashimoto, D., Lucas, D., Kunisaki, Y., Pinho, S., Leboeuf, M., Noizat, C., van Rooijen, N., Tanaka, M., Zhao, Z. J., Bergman, A., Merad, M., and Frenette, P. S. (2013) CD169(+) macrophages provide a niche promoting erythropoiesis under homeostasis and stress. *Nat. Med.* **19,** 429–436
6. Chow, A., Lucas, D., Hidalgo, A., Méndez-Ferrer, S., Hashimoto, D., Scheiermann, C., Battista, M., Leboeuf, M., Prophete, C., van Rooijen, N., Tanaka, M., Merad, M., and Frenette, P. S. (2011) Bone marrow CD169+ macrophages promote the retention of hematopoietic stem and progenitor cells in the mesenchymal stem cell niche. *J. Exp. Med.* **208,** 261–271
7. Crocker, P. R., Werb, Z., Gordon, S., and Bainton, D. F. (1990) Ultrastructural localization of a macrophage-restricted sialic acid binding hemagglutinin, SER, in macrophage-hematopoietic cell clusters. *Blood* **76,** 1131–1138
8. Oetke, C., Vinson, M. C., Jones, C., and Crocker, P. R. (2006) Sialoadhesin-deficient mice exhibit subtle changes in B- and T-cell populations and reduced immunoglobulin M levels. *Mol. Cell. Biol.* **26,** 1549–1557
9. Hartnell, A. (2001) Characterization of human sialoadhesin, a sialic acid binding receptor expressed by resident and inflammatory macrophage populations. *Blood* **97,** 288–296
10. Iannacone, M., Moseman, E. A., Tonti, E., Bosurgi, L., Junt, T., Henrickson, S. E., Whelan, S. P., Guidotti, L. G., and von Andrian, U. H. (2010) Subcapsular sinus macrophages prevent CNS invasion on peripheral infection with a neurotropic virus. *Nature* **465,** 1079–1083
11. Junt, T., Moseman, E. A., Iannacone, M., Massberg, S., Lang, P. A., Boes, M., Fink, K., Henrickson, S. E., Shayakhmetov, D. M., Di Paolo, N. C., van Rooijen, N., Mempel, T. R., Whelan, S. P., and von Andrian, U. H. (2007) Subcapsular sinus macrophages in lymph nodes clear lymph-borne viruses and present them to antiviral B cells. *Nature* **450,** 110–114
12. Prather, R. S., Rowland, R. R., Ewen, C., Trible, B., Kerrigan, M., Bawa, B., Teson, J. M., Mao, J., Lee, K., Samuel, M. S., Whitworth, K. M., Murphy, C. N., Egen, T., and Green, J. A. (2013) An intact sialoadhesin (Sn/SIGLEC1/CD169) is not required for attachment/internalization of the

porcine reproductive and respiratory syndrome virus. *J. Virol.* **87,** 9538–9546
13. Puryear, W. B., Akiyama, H., Geer, S. D., Ramirez, N. P., Yu, X., Reinhard, B. M., and Gummuluru, S. (2013) Interferon-inducible mechanism of dendritic cell-mediated HIV-1 dissemination is dependent on Siglec-1/CD169. *PLoS Pathog.* **9,** e1003291
14. Vinson, M., van der Merwe, P. A., Kelm, S., May, A., Jones, E. Y., and Crocker, P. R. (1996) Characterization of the sialic acid-binding site in sialoadhesin by site-directed mutagenesis. *J. Biol. Chem.* **271,** 9267–9272
15. May, A. P., Robinson, R. C., Vinson, M., Crocker, P. R., and Jones, E. Y. (1998) Crystal structure of the N-terminal domain of sialoadhesin in complex with 3′ sialyl-lactose at 1.85 A resolution. *Mol. Cell* **1,** 719–728
16. Gagiannis, D., Gossrau, R., Reutter, W., Zimmermann-Kordmann, M., and Horstkorte, R. (2007) Engineering the sialic acid in organs of mice using *N*-propanoylmannosamine. *Biochim. Biophys. Acta* **1770,** 297–306
17. Kelm, S., Brossmer, R., Isecke, R., Gross, H. J., Strenge, K., and Schauer, R. (1998) Functional groups of sialic acids involved in binding to siglecs (sialoadhesins) deduced from interactions with synthetic analogues. *Eur. J. Biochem.* **255,** 663–672
18. Kelm, S., Schauer, R., Manuguerra, J. C., Gross, H. J., and Crocker, P. R. (1994) Modifications of cell surface sialic acids modulate cell adhesion mediated by sialoadhesin and CD22. *Glycoconj. J.* **11,** 576–585
19. Izquierdo-Useros, N., Lorizate, M., Contreras, F. X., Rodriguez-Plata, M. T., Glass, B., Erkizia, I., Prado, J. G., Casas, J., Fabriàs, G., Kräusslich, H. G., and Martinez-Picado, J. (2012) Sialyllactose in viral membrane gangliosides is a novel molecular recognition pattern for mature dendritic cell capture of HIV-1. *PLoS Biol.* **10,** e1001315
20. Puryear, W. B., Yu, X., Ramirez, N. P., Reinhard, B. M., and Gummuluru, S. (2012) HIV-1 incorporation of host-cell-derived glycosphingolipid GM3 allows for capture by mature dendritic cells. *Proc. Natl. Acad. Sci. U.S.A.* **109,** 7475–7480
21. Kayser, H., Zeitler, R., Kannicht, C., Grunow, D., Nuck, R., and Reutter, W. (1992) Biosynthesis of a nonphysiological sialic acid in different rat organs, using *N*-propanoyl-D-hexosamines as precursors. *J. Biol. Chem.* **267,** 16934–16938
22. Mahal, L. K., Yarema, K. J., and Bertozzi, C. R. (1997) Engineering chemical reactivity on cell surfaces through oligosaccharide biosynthesis. *Science* **276,** 1125–1128
23. Keppler, O. T., Horstkorte, R., Pawlita, M., Schmidt, C., and Reutter, W. (2001) Biochemical engineering of the *N*-acyl side chain of sialic acid: biological implications. *Glycobiology* **11,** 11R-18R
24. Horstkorte, R., Rau, K., Laabs, S., Danker, K., and Reutter, W. (2004) Biochemical engineering of the *N*-acyl side chain of sialic acid leads to increased calcium influx from intracellular compartments and promotes differentiation of HL60 cells. *FEBS Lett.* **571,** 99–102
25. Keppler, O. T., Herrmann, M., von der Lieth, C. W., Stehling, P., Reutter, W., and Pawlita, M. (1998) Elongation of the *N*-acyl side chain of sialic acids in MDCK II cells inhibits influenza A virus infection. *Biochem. Biophys. Res. Commun.* **253,** 437–442
26. Keppler, O. T., Stehling, P., Herrmann, M., Kayser, H., Grunow, D., Reutter, W., and Pawlita, M. (1995) Biosynthetic modulation of sialic acid-dependent virus-receptor interactions of two primate polyoma viruses. *J. Biol. Chem.* **270,** 1308–1314
27. Wieser, J. R., Heisner, A., Stehling, P., Oesch, F., and Reutter, W. (1996) *In vivo* modulated *N*-acyl side chain of *N*-acetylneuraminic acid modulates the cell contact-dependent inhibition of growth. *FEBS Lett.* **395,** 170–173
28. Saxon, E., and Bertozzi, C. R. (2000) Cell surface engineering by a modified Staudinger reaction. *Science* **287,** 2007–2010
29. Krieger, E., Darden, T., Nabuurs, S. B., Finkelstein, A., and Vriend, G. (2004) Making optimal use of empirical energy functions: force-field parameterization in crystal space. *Proteins* **57,** 678–683
30. Jin, J., Li, F., and Mothes, W. (2011) Viral determinants of polarized assembly for the murine leukemia virus. *J. Virol.* **85,** 7672–7682
31. Pizzato, M., Erlwein, O., Bonsall, D., Kaye, S., Muir, D., and McClure, M. O. (2009) A one-step SYBR Green I-based product-enhanced reverse transcriptase assay for the quantitation of retroviruses in cell culture supernatants. *J. Virol. Methods* **156,** 1–7
32. Duan, Y., Wu, C., Chowdhury, S., Lee, M. C., Xiong, G., Zhang, W., Yang, R., Cieplak, P., Luo, R., Lee, T., Caldwell, J., Wang, J., and Kollman, P. (2003) A point-charge force field for molecular mechanics simulations of proteins based on condensed-phase quantum mechanical calculations. *J. Comput. Chem.* **24,** 1999–2012
33. Jakalian, A., Jack, D. B., and Bayly, C. I. (2002) Fast, efficient generation of high-quality atomic charges. AM1-BCC model: II. Parameterization and validation. *J. Comput. Chem.* **23,** 1623–1641
34. Shan, Y., Klepeis, J. L., Eastwood, M. P., Dror, R. O., and Shaw, D. E. (2005) Gaussian split Ewald: A fast Ewald mesh method for molecular simulation. *J. Chem. Phys.* **122,** 54101
35. Wang, J., Wolf, R. M., Caldwell, J. W., Kollman, P. A., and Case, D. A. (2004) Development and testing of a general amber force field. *J. Comput. Chem.* **25,** 1157–1174
36. Naito-Matsui, Y., Takada, S., Kano, Y., Iyoda, T., Sugai, M., Shimizu, A., Inaba, K., Nitschke, L., Tsubata, T., Oka, S., Kozutsumi, Y., and Takematsu, H. (2014) Functional evaluation of activation-dependent alterations in the sialoglycan composition of T cells. *J. Biol. Chem.* **289,** 1564–1579
37. Rarey, M., Kramer, B., Lengauer, T., and Klebe, G. (1996) A fast flexible docking method using an incremental construction algorithm. *J. Mol. Biol.* **261,** 470–489
38. Schneider, N., Lange, G., Hindle, S., Klein, R., and Rarey, M. (2013) A consistent description of HYdrogen bond and DEhydration energies in protein-ligand complexes: methods behind the HYDE scoring function. *J. Comput. Aided Mol. Des.* **27,** 15–29
39. Inoue, S., and Inoue, Y. (2003) Ultrasensitive analysis of sialic acids and oligo/polysialic acids by fluorometric high-performance liquid chromatography. *Methods Enzymol.* **362,** 543–560
40. Galuska, S. P., Geyer, H., Weinhold, B., Kontou, M., Röhrich, R. C., Bernard, U., Gerardy-Schahn, R., Reutter, W., Münster-Kühnel, A., and Geyer, R. (2010) Quantification of nucleotide-activated sialic acids by a combination of reduction and fluorescent labeling. *Anal. Chem.* **82,** 4591–4598
41. Smith, D. F., and Prieto, P. A. (2001) Special considerations for glycolipids and their purification. *Curr. Protoc. Mol. Biol.* Chapter 17, Unit 17.13
42. Wratil, P. R., Rigol, S., Solecka, B., Kohla, G., Kannicht, C., Reutter, W., Giannis, A., and Nguyen, L. D. (2014) A novel approach to decrease sialic acid expression in cells by a C-3-modified *N*-acetylmannosamine. *J. Biol. Chem.* **289,** 32056–32063
43. Lewis, P. F., and Emerman, M. (1994) Passage through mitosis is required for oncoretroviruses but not for the human immunodeficiency virus. *J. Virol.* **68,** 510–516
44. Roe, T., Reynolds, T. C., Yu, G., and Brown, P. O. (1993) Integration of murine leukemia virus DNA depends on mitosis. *EMBO J.* **12,** 2099–2108
45. Kuka, M., and Iannacone, M. (2014) The role of lymph node sinus macrophages in host defense. *Ann. N.Y. Acad. Sci.* **1319,** 38–46
46. Posch, W., Steger, M., Knackmuss, U., Blatzer, M., Baldauf, H. M., Doppler, W., White, T. E., Hörtnagl, P., Diaz-Griffero, F., Lass-Flörl, C., Hackl, H., Moris, A., Keppler, O. T., and Wilflingseder, D. (2015) Complement-opsonized HIV-1 overcomes restriction in dendritic cells. *PLoS Pathog.* **11,** e1005005
47. Coutinho, A., and Möller, G. (1973) B cell mitogenic properties of thymus-independent antigens. *Nat. New Biol.* **245,** 12–14
48. Dwyer, J. M., and Johnson, C. (1981) The use of concanavalin A to study the immunoregulation of human T cells. *Clin. Exp. Immunol.* **46,** 237–249
49. Luchansky, S. J., and Bertozzi, C. R. (2004) Azido sialic acids can modulate cell-surface interactions. *Chembiochem* **5,** 1706–1709
50. Brügger, B., Glass, B., Haberkant, P., Leibrecht, I., Wieland, F. T., and Kräusslich, H. G. (2006) The HIV lipidome: a raft with an unusual composition. *Proc. Natl. Acad. Sci. U.S.A.* **103,** 2641–2646
51. Chan, R., Uchil, P. D., Jin, J., Shui, G., Ott, D. E., Mothes, W., and Wenk, M. R. (2008) Retroviruses human immunodeficiency virus and murine leukemia virus are enriched in phosphoinositides. *J. Virol.* **82,** 11228–11238
52. Sonnenburg, J. L., Altheide, T. K., and Varki, A. (2004) A uniquely human consequence of domain-specific functional adaptation in a sialic acid-binding receptor. *Glycobiology* **14,** 339–346
53. Oetke, C., Hinderlich, S., Brossmer, R., Reutter, W., Pawlita, M., and Kep-

pler, O. T. (2001) Evidence for efficient uptake and incorporation of sialic acid by eukaryotic cells. *Eur. J. Biochem.* **268,** 4553–4561
54. Rosenberg, N., and Jolicoeur, P. (1997) in *Retroviruses* (Coffin, J. M., Hughes, S. H., and Varmus, H. E., eds) pp. 475–586, Cold Spring Harbor Laboratory Press, Cold Spring Harbor, NY
55. Banchereau, J., and Steinman, R. M. (1998) Dendritic cells and the control of immunity. *Nature* **392,** 245–252
56. Geijtenbeek, T. B., Kwon, D. S., Torensma, R., van Vliet, S. J., van Duijnhoven, G. C., Middel, J., Cornelissen, I. L., Nottet, H. S., KewalRamani, V. N., Littman, D. R., Figdor, C. G., and van Kooyk, Y. (2000) DC-SIGN, a dendritic cell-specific HIV-1-binding protein that enhances trans-infection of T cells. *Cell* **100,** 587–597
57. Geijtenbeek, T. B., Torensma, R., van Vliet, S. J., van Duijnhoven, G. C., Adema, G. J., van Kooyk, Y., and Figdor, C. G. (2000) Identification of DC-SIGN, a novel dendritic cell-specific ICAM-3 receptor that supports primary immune responses. *Cell* **100,** 575–585
58. Kwon, D. S., Gregorio, G., Bitton, N., Hendrickson, W. A., and Littman, D. R. (2002) DC-SIGN-mediated internalization of HIV is required for trans-enhancement of T cell infection. *Immunity* **16,** 135–144
59. Garcia, E., Pion, M., Pelchen-Matthews, A., Collinson, L., Arrighi, J. F., Blot, G., Leuba, F., Escola, J. M., Demaurex, N., Marsh, M., and Piguet, V. (2005) HIV-1 trafficking to the dendritic cell-T-cell infectious synapse uses a pathway of tetraspanin sorting to the immunological synapse. *Traffic* **6,** 488–501
60. Cavrois, M., Neidleman, J., Kreisberg, J. F., and Greene, W. C. (2007) *In vitro* derived dendritic cells trans-infect CD4 T cells primarily with surface-bound HIV-1 virions. *PLoS Pathog.* **3,** e4
61. Akiyama, H., Ramirez, N. G., Gudheti, M. V., and Gummuluru, S. (2015) CD169-mediated trafficking of HIV to plasma membrane invaginations in dendritic cells attenuates efficacy of anti-gp120 broadly neutralizing antibodies. *PLoS Pathog.* **11,** e1004751
62. Yu, H. J., Reuter, M. A., and McDonald, D. (2008) HIV traffics through a specialized, surface-accessible intracellular compartment during trans-infection of T cells by mature dendritic cells. *PLoS Pathog.* **4,** e1000134
63. Pino, M., Erkizia, I., Benet, S., Erikson, E., Fernández-Figueras, M. T., Guerrero, D., Dalmau, J., Ouchi, D., Rausell, A., Ciuffi, A., Keppler, O. T., Telenti, A., Kräusslich, H. G., Martinez-Picado, J., and Izquierdo-Useros, N. (2015) HIV-1 immune activation induces Siglec-1 expression and enhances viral trans-infection in blood and tissue myeloid cells. *Retrovirology* **12,** 37
64. Izquierdo-Useros, N., Esteban, O., Rodriguez-Plata, M. T., Erkizia, I., Prado, J. G., Blanco, J., García-Parajo, M. F., and Martinez-Picado, J. (2011) Dynamic imaging of cell-free and cell-associated viral capture in mature dendritic cells. *Traffic* **12,** 1702–1713
65. Brinkman-Van der Linden, E. C., Sjoberg, E. R., Juneja, L. R., Crocker, P. R., Varki, N., and Varki, A. (2000) Loss of *N*-glycolylneuraminic acid in human evolution. Implications for sialic acid recognition by siglecs. *J. Biol. Chem.* **275,** 8633–8640
66. Naito, Y., Takematsu, H., Koyama, S., Miyake, S., Yamamoto, H., Fujinawa, R., Sugai, M., Okuno, Y., Tsujimoto, G., Yamaji, T., Hashimoto, Y., Itohara, S., Kawasaki, T., Suzuki, A., and Kozutsumi, Y. (2007) Germinal center marker GL7 probes activation-dependent repression of *N*-glycolylneuraminic acid, a sialic acid species involved in the negative modulation of B-cell activation. *Mol. Cell. Biol.* **27,** 3008–3022
67. Goffinet, C., Michel, N., Allespach, I., Tervo, H-M., Hermann, V., Kräusslich, H-G., Greene, W. C., and Keppler, O. T. (2007) Primary T-cells from human CD4/CCR5-transgenic rats support all early steps of HIV-1 replication including integration, but display impaired viral gene expression *Retrovirology* **4,** 53